Available online at www.sciencedirect.com
SCIENCE DIRECT
Journal of Sound and Vibration 297 (2006) 1–16
JOURNAL OF SOUND AND VIBRATION
www.elsevier.com/locate/jsvi

A method for detecting damage-induced nonlinearities in structures using information theory

J.M. Nichols[a,*], M. Seaver[a], S.T. Trickey[a]

[a]*Naval Research Laboratory, 4555 Overlook Avenue Washington, DC 20375, USA*

Received 3 January 2005; received in revised form 18 July 2005; accepted 6 January 2006

Abstract

In this work a new approach is presented for detecting the presence of damage-induced nonlinearities in structures from measurements of structural dynamics. Two different information-theoretic (IT) measures, the time-delayed mutual information and the time-delayed transfer entropy are used to provide a probabilistic measure of the coupling between structural components. These measures may be used to capture both linear and nonlinear relationships among time-series data. The formula for both quantities is derived for a linear, five degree-of-freedom system subject to Gaussian excitation. An algorithm is then described for computing the IT metrics from time-series data and results are shown to agree with theory. We then show that as the coupling between the structure's components changes from linear to nonlinear the "information flow" can be used to indicate the degree of nonlinearity. Deviations from a linear model are quantified statistically by generating surrogate data sets that, by construction, possess only linear (second-order) correlations. We then apply the proposed algorithms to both the original data and the surrogates. Differences in the results are shown to be proportional to the degree of nonlinearity. This result is shown to be independent of global changes in stiffness and is therefore unaffected by certain models of environmental variability. Furthermore, the method provides an absolute measure of nonlinearity and therefore does not require a baseline data set for making comparisons. This approach is discussed in the context of structural health monitoring where damage is often associated with structural nonlinearity.

1. Introduction

Vibration-based structural health monitoring (SHM) focuses on drawing inferences about the health of a structure from the structure's dynamic response to ambient or applied excitation. The practitioner collects data from an undamaged structure, forms a baseline set of metrics or "features", and then tracks the evolution of those metrics. Feature values that are statistically different from the baseline values are presumed to be indicative of damage. Two primary obstacles are the need for baseline data and the difficulty in separating changes in feature values due to environmental variability from those due to damage. Many, if not most situations call for the practitioner to monitor an existing structure without the benefit of a baseline set of structural response data. It is therefore desirable to develop an approach that can detect *absolute* damage with

*Corresponding author. Tel.: +202 404 5433; fax: +202 767 5792.
E-mail address: jonathan.nichols@nrl.navy.mil (J.M. Nichols).

0022-460X/$ - see front matter © 2006 Elsevier Ltd. All rights reserved.
doi:10.1016/j.jsv.2006.01.025

a minimal number of assumptions. Changes in feature value due to ambient conditions (e.g. temperature) further complicate the process. For example, temperature fluctuations can cause large changes in the measured natural frequencies of a structure. A bridge monitoring study by Peeters et al. [1] found that temperature alone caused the eigenfrequencies of the Z24 bridge in Switzerland to change by as much as 18%.

Damage in structures is frequently modeled as the introduction of a nonlinearity into an a structure or structural component that is otherwise (in a healthy state) accurately described by a linear model [2,3]. Such mechanisms might include the presence of a crack (bi-linear stiffness), post-buckled behavior (Duffing nonlinearity) and/or bolt rattling (impacting, stick-slip). Here we present an approach for detecting damage-induced nonlinearities in a structure based on its vibrational response. Specifically we test whether or not the observed data are consistent with the hypothesis of a linear stochastic process (i.e. a healthy structure produced them). The approach yields an absolute measure of nonlinearity and therefore does not require an explicit measurement of the healthy structure's dynamics. Furthermore, the approach will be shown to be insensitive to global changes in stiffness such as those caused by temperature fluctuations. While stiffness changes may alter global system properties (e.g. modal properties) they do not necessarily change the form of the underlying model (e.g. linear vs. nonlinear). The proposed approach targets the presence of nonlinearity and is therefore not affected by this type of variability.

Many of the standard signal processing tools (e.g. frequency response functions) assume the underlying system is linear and are thus unable to directly capture nonlinear relationships among time-series data. Instead, nonlinearity will manifest itself as a breakdown in the ability of many linear time-series analysis techniques to accurately describe the dynamics, i.e. a distortion [4]. This "deviation from linearity" could conceivably be taken as a measure reflecting the degree of nonlinearity, however this requires some a priori knowledge of the system under study, i.e. we need to know how the distortion will manifest itself. Perhaps the most straightforward approach to nonlinearity detection is to apply varying load levels to the structure and search for amplitude dependence in the frequency response. This technique may pose practical issues if variable amplitude loading is unavailable. A more sophisticated approach is to use time-frequency analysis to search for amplitude dependence in the structures parameters. This general approach to detecting damage-induced nonlinearities was employed by Neild et al. [5]. Feldman [6] used the Hilbert transform to identify "backbone" curves associated with a free-decay response for oscillators with various nonlinearities. The method was further extended to forced vibration [7] and later applied to damage detection in rotors [8]. If one knows how a certain nonlinearity will affect this backbone the approach could be used to yield a direct measure of nonlinearity without necessarily requiring a baseline. It is unclear, however, how deviations from a healthy model (backbone) are to be quantified or how the approach would perform in the absence of a well-defined model (i.e. where multiple nonlinearities/damages are present). The practitioner essentially has to make a judgment as to what level of nonlinearity is significant thus making an automated health monitoring scheme difficult to implement. Furthermore, this approach was designed for monocomponent signals (single harmonic) derived from a single degree-of-freedom (dof) system or from an appropriately filtered multi-dof system thus limiting practicality in many situations. A similar approach was followed in Ref. [9] using the wavelet transform. This approach is well suited to multi-dof systems but was designed to work with impulse excitation and still requires user judgement as to the significance of the observed nonlinearity. Another approach to nonlinear system identification was recently proposed by Kerschen et al. [10]. This approach is based on Bayesian model selection and also requires a priori knowledge of an underlying model or class of models to be tested. A different approach is to use higher-order spectra to assess the presence of nonlinearity. For example, one might use the bi-spectrum to detect nonlinear coupling in various frequency components [4]. Higher-order approaches can capture certain types of nonlinearity but are not generic in the sense that they still focus on a specific type of correlation.

Rather than modifying linear signal processing tools and/or methods, the approach described herein was designed specifically to explore nonlinear relationships among time-series data. The method does not require a specific model of the nonlinearity, works for any type of stationary excitation, and requires no pre-processing (e.g. filtering) of the response time series. Furthermore, by using the method of surrogate data the diagnosis may be made in a reliable, statistically significant fashion. In the absence of a priori knowledge of a specific damage mechanism (nonlinearity), surrogate data provide a data-driven baseline leading to an absolute measure of damage.

Two different information-theoretic (IT) measures are presented, the *time-delayed mutual information*, and the *time-delayed transfer entropy*. These metrics have seen use in the physics literature but their utility in analyzing structural dynamics has not yet been explored. Both quantities have their roots in information theory and are designed to measure the co-dependence of dynamical variables in a probabilistic sense. Rather than considering only second-order correlations in the data (e.g. linear cross-correlation) these metrics are designed to consider the entire probability distribution of the signal(s), regardless of their underlying form, and hence the higher-order correlations associated with nonlinearity. Our general approach consists of first constructing surrogate data sets from the original structural response data. These surrogates are designed to match exactly the linear auto- and cross-correlations among the data. We then compute the ITs on both the original data and the surrogates and search for discrepancies. The surrogate data effectively serve as a "bootstrapped" baseline data set that allow us to quantitatively test against the hypothesis of a linear structure. We argue that ITs provide an appropriate framework for studying nonlinear coupling as they make no assumptions about the underlying model.

Sections 2 and 3 describe the time-delayed mutual information and time-delayed transfer entropy, respectively. In the case of linear coupling both quantities are shown to reduce to a simple function of the dynamic, linear cross-correlation coefficient between the structure's variables. An algorithm for estimating both metrics from time-series data is presented in Section 4. The approach relies on a kernel density estimation technique for approximating the various probabilities required by both metrics. The procedure for generating the surrogate data sets is also described in Section 5. We then derive an analytical expression for both quantities in Section 6 and compare times-series estimates to theoretical predictions. Finally, we demonstrate the power of the proposed approach by detecting the presence and degree of nonlinearity in a 5 dof structure subject to Gaussian excitation. Ambient conditions are varied, simulating a temperature gradient on the structure. The proposed approach is unaffected by this variation and correctly identifies the presence of the nonlinearity.

2. Time-delayed mutual information

Assume we can monitor the dynamics of a spatially extended system by recording the system output from L different locations at N discrete points in time resulting in the multi-variate time series $\mathbf{x}(n) \equiv x_i(n)$ $i = 1, \ldots, L$ $n = 1 \ldots N$ (we use boldface type to denote a vector). In order to draw inference about the coupling mechanisms in a system we are effectively asking questions about the relationship(s) $x_i(n) = f_i(\mathbf{x}(n)) \in L$. In structural dynamics, if the function(s) f_i are linear there exist a variety of signal processing techniques i capable of extracting the relevant parameters, e.g. stiffness, damping, etc. The linear cross-correlation and transfer function estimates are two frequently used approaches. While computationally efficient, these techniques are by definition only capable of exploring a specific kind of relationship in the data. These methods assume that all of the relevant information is contained in second-order correlations, i.e. the covariance matrix. A more general way to study the properties of the f_i is to ask how much information the two signals $x_i(n), x_j(n)$ have in common and how that information varies in time (flows) between locations i and j. Each measurement can be thought of as a random variable with underlying probability density function $p(x_i(n))$ and joint probability density $p(x_i(n), x_j(m))$. In the development that follows we assume stationarity such that $p(x_i(n)) = p(x_i(n+k)) \equiv p(x_i)$, i.e. a time shift does not affect the probability density function. Similarly for joint densities $p(x_i(n), x_j(m)) = p(x_i(n+k), x_j(m+k)) \equiv p(x_i, x_j(m-n))$, i.e. only relative lags (advances) matter. This assumption is made for purely for practical reasons. In order to estimate probability densities from a single observed time series (see Section 4) we will need to assume stationarity and ergodicity.

If the processes are statistically independent (uncoupled) $p(x_i, x_j) = p(x_i)p(x_j)$, that is the joint probability density is the product of the two individual probability densities. In order to quantify the degree of independence one may compute the mutual information

$$I(x_i; x_j) = \int \int p(x_i, x_j) \log\left(\frac{p(x_i, x_j)}{p(x_i)p(x_j)}\right) \mathrm{d}x_i \, \mathrm{d}x_j \tag{1}$$

which effectively maps deviations from the assumption of independence to a scalar. The integrals in Eq. (1) are taken over all possible states $x_i(n), x_j(n)$. Another interpretation of Eq. (1) is a "distance from independence".

The mutual information function is strictly non-negative and it is assumed that $0\log(0) = 0$. This quantity has seen use in a variety of fields, most notably in nonlinear dynamics for selecting the delay for time series embedding [11]. Other applications have included the selection of location for sensor placement [12] in SHM, in communications [13], and as a "contrast function" for performing independent component analysis [14].

If one seeks to study how information moves from i to j one can add a time delay in one of the variables. Denote $p(x_i, x_j(T))$ as the joint probability density associated with considering the delayed time series $x_j(n+T)$ in place of $x_j(m)$ (i.e. $T = m - n$). The average mutual information function then reads

$$I(x_i; x_j, T) = \int\int p(x_i, x_j(T))\log_2\left(\frac{p(x_i, x_j(T))}{p(x_i)p(x_j(T))}\right) \mathrm{d}x_i\,\mathrm{d}x_j. \tag{2}$$

This quantity was used by Vastano and Swinney [15] as a means of studying information transport in spatially extended systems. If information present at location i is transmitted to location j there will be a peak in the curve $I(x_i; x_j(T))$ at $T>0$ as the joint probability density increases and reaches its maximum. A peak that occurs for $T<0$ implies that the information is being transported from j to i. Time-delayed mutual information has been used to detect the direction of information flow in neuron firings [16], in a reaction–diffusion system [15], a coupled map lattice [17], and more recently in population dynamics [18]. For estimation purposes it will be convenient to expand Eq. (2) into entropy form

$$\begin{aligned} I(x_i; x_j, T) = &\int\int p(x_i, x_j(T))\log_2(p(x_i, x_j(T)))\,\mathrm{d}x_i\,\mathrm{d}x_j(T) - \int p(x_i)\log_2(p(x_i))\,\mathrm{d}x_i \\ &- \int p(x_j(T))\log_2(p(x_j(T)))\,\mathrm{d}x_j(T), \end{aligned} \tag{3}$$

where $\int p(a)\log_2(p(a))$ and $\int\int p(a,b)\log_2(p(a,b))$ are the Shannon entropies associated with the single and joint distributions of random variables a, b.

Assume the two processes x_i, x_j are zero-mean, Gaussian distributed with variances $\sigma_{x_i}^2$, $\sigma_{x_j}^2$ and dynamic cross-correlation coefficient $\rho_{x_i x_j}(T)$. Carrying out the integration required by Eq. (3) yields

$$I(x_i; x_j, T) = -\tfrac{1}{2}\log(1 - \rho_{x_i x_j}^2(T)). \tag{4}$$

Eq. (4) is referred to as the "linearized" information flow between the two processes x_i and x_j and considers only second moments in the data. In this special case all of the information shared between the two processes can be captured by the linear cross-correlation coefficient. For the general case described by Eq. (2), however, the information flow $I(x_i; x_j, T)$ may be thought of as a *nonlinear* cross-correlation function capable of capturing both linear and nonlinear (higher-order) correlations in time-series data. The algorithm required for evaluating Eq. (2) is given in Section 4.

3. Transfer entropy

One potential drawback of using the mutual information function to measure coupling is that it does not consider the dynamics of the underlying processes explicitly. Rather, one has to introduce a time delay in order to explore dynamic correlations. More recently a different metric, the transfer entropy, has been introduced by Schreiber [19] and incorporates the dynamic nature of the processes directly. The transfer entropy metric was designed specifically to look at information transport and has been used already in examining physiological coupling [20] and financial time series [21]. Rather than focusing on the joint probability density, transfer entropy includes the notion of conditional probability. If the probability of a random variable having a given value at discrete time $n+1$ is conditional on the previous k values only, the dynamics of that variable are said to be described by a kth order Markov process. Mathematically this means the transition probabilities follow $p(x_i(n+1)|x_i(n), x_i(n-1), \ldots, x_i(n-k+1)) = p(x_i(n+1)|x_i(n), x_i(n-1), \ldots, x_i(n-k+1), x_i(n-k))$, that is to say the dynamics at discrete time $n+1$) is independent of the dynamics at time $n-k$. Assuming stationarity (absolute time index does not matter) we may define $p(x_i(1)|x_i^{(k)}) \equiv p(x_i(n+1)|x_i(n), x_i(n-1), x_i(n-2), \ldots, x_i(n-k+1))$. If two processes are being considered one could ask how the dynamics of x_j influence these transition probabilities. In other words, explore the possibility that the dynamics follow

$p(x_i(n+1)|x_i(n), x_i(n-1), \ldots, x_i(n-k+1), (x_j(m), x_j(m-1), \ldots, x_j(m-l+1))$ or in the more compact notation $p(x_i(1)|x_i^{(k)}, x_j^{(l)}(m-n))$ (again we have assumed stationarity such that only time lags/advances are relevant). Here the dynamics of x_j are modeled as a lth order Markov process. The probability of the process x_i being in a given state at time $n+1$ is dependent on past history *and* values of the process x_j at discrete time $m, m-1, \ldots, m-l+1$.

Based on this description of the dynamics, we may define two processes to be coupled if one influences the transition probabilities of the other. The degree of influence can be quantified in the same way as for mutual information. Following Schreiber [19] and denoting $T = m - n$ we write

$$T(x_i(1)|x_i^{(k)}, x_j^{(l)}) = \int\int\int p(x_i(1), x_i^{(k)}, x_j^{(l)}(T)) \log_2 \left(\frac{p(x_i(1)|x_i^{(k)}, x_j^{(l)}(T))}{p(x_i(1)|x_i^{(k)})} \right) \mathrm{d}x_i(1)\, \mathrm{d}x_i^{(k)}\, \mathrm{d}x_j^{(l)}(T) \tag{5}$$

as the time-delayed transfer entropy. While mutual information measures a distance from the hypothesis of statistical independence, transfer entropy measures a distance from the hypothesis that the dynamics of $x_i(n)$ can be described entirely by its past history and that no new information is gained by considering the dynamics of $x_j(n+T)$. Making use of the law of conditional probabilities $p(a|b) = p(a,b)/p(b)$ and expanding Eq. (5) may be re-written in entropy form as

$$\begin{aligned} T(x_i(1)|x_i^{(k)}, x_j^{(l)}) = & \int\int\int p(x_i(1), x_i^{(k)}, x_j^{(l)}(T)) \log_2 \left(p(x_i(1), x_i^{(k)}, x_j^{(l)}(T))\right) \mathrm{d}x_i(1)\, \mathrm{d}x_i^{(k)}\, \mathrm{d}x_j^{(l)}(T) \\ & + \int p(x_i^{(k)}) \log_2 \left(p(x_i^{(k)})\right) \mathrm{d}x_i^{(k)} - \int\int p(x_i^{(k)}, x_j^{(l)}(T)) \\ & \times \log_2 \left(p(x_i^{(k)}, x_j^{(l)}(T))\right) \mathrm{d}x_i^{(k)}\, \mathrm{d}x_j^{(l)}(T) \\ & - \int\int p(x_i(1), x_i) \log_2 \left(p(x_i(1), x_i)\right) \mathrm{d}x_i(1)\, \mathrm{d}x_i^{(k)}. \end{aligned} \tag{6}$$

Should consideration of $x_j(n+T)$ provide no additional knowledge about the dynamics of $x_i(n)$ the transfer entropy will be zero, rising to some positive value should $x_j(n+T)$ carry information not possessed in $x_i(n)$. Several free parameters exist in Eq. (6), most notably the assumed order of the processes k, l. In this work we assume $k = l = 1$ for simplicity and instead focus on varying the time delay $T = m - n$ in an effort to see how much information $x_j(n+T)$ carries about $x_i(n)$ over various time scales.

For linear, Gaussian processes the transfer entropy between masses i, j can be written in terms of the covariance matrices associated with its arguments as [20]

$$T(x_i(1)|x_i, x_j(T)) = \frac{1}{2} \log \left(\frac{|\mathscr{C}_{x_i(1), x_i, x_j(T)}||\mathscr{C}_{x_i}|}{|\mathscr{C}_{x_i, x_j(T)}||\mathscr{C}_{x_i(1), x_i}|} \right), \tag{7}$$

where

$$\mathscr{C}_{x_i(1), x_i, x_j(T)} = \begin{bmatrix} E[x_i(n+1)x_i(n+1)] & E[x_i(n+1)x_i(n)] & E[x_i(n+1)x_j(n+T)] \\ E[x_i(n)x_i(n+1)] & E[x_i(n)x_i(n)] & E[x_i(n)x_j(n+T)] \\ E[x_j(n+T)x_i(n+1)] & E[x_j(n+T)x_i(n)] & E[x_j(n+T)x_j(n+T)] \end{bmatrix},$$

$$\mathscr{C}_{x_i(1), x_i} = \begin{bmatrix} E[x_i(n+1)x_i(n+1)] & E[x_i(n+1)x_i(n)] \\ E[x_i(n)x_i(n+1)] & E[x_i(n)x_i(n)] \end{bmatrix},$$

and

$$\mathscr{C}_{x_i, x_j(T)} = \begin{bmatrix} E[x_i(n)x_i(n)] & E[x_i(n)x_j(n+T)] \\ E[x_j(n+T)x_i(n)] & E[x_j(n+T)x_j(n+T)] \end{bmatrix}$$

and $E[\cdot]$ takes the expected value. The determinant of $\mathscr{C}_{x_i}$ is simply the variance $E[x_i(n)x_i(n)] = \sigma_{x_i}^2$. The other expected values may also be computed, assuming stationarity, to give the linearized transfer entropy. Define the linear cross-correlation between the stationary time series x_i, x_j as $R_{x_ix_j}(T) \equiv E[x_i(n)x_j(n+T)]$. For $i=j$ one has the autocorrelation $R_{x_ix_i}(T)$. For convenience these quantities are normalized by the signal variance(s). Therefore denote $\hat{R}_{x_ix_i}(T) \equiv R_{x_ix_i}(T)/R_{x_ix_i}(0)$ as the normalized auto-correlation. The linear cross-correlation coefficient $\rho_{x_ix_j}(T) = R_{x_ix_j}(T)/\sqrt{R_{x_ix_i}(0)R_{x_jx_j}(0)}$ has already been referred to in the previous section (Eq. (4)). The quantities involving discrete time $n+1$ are obtained by noting that $E[x_i(n+1)x_i(n)] = R_{x_ix_i}(1)$ and $E[x_i(n+1)x_j(n+T)] = R_{x_ix_j}(T-1)$. Correlations associated with negative delays are obtained by the general relationship $R_{x_ix_j}(-T) = R_{x_jx_i}(T)$. Computing Eq. (7) therefore requires not only the dynamic linear auto- and cross-correlation coefficients, but also their time-shifted versions. Using this notation, Eq. (7) becomes

$$T(x_i(1)|x_i, x_j(T)) = \frac{1}{2}\log_2\left\{\frac{-(-1+\rho_{x_ix_j}^2(T))(\hat{R}_{x_ix_i}^2(1)-1)}{-2\rho_{x_ix_j}(T-1)\hat{R}_{x_ix_i}(1)\rho_{x_ix_j}(T)+\rho_{x_ix_j}^2(T-1)+(\hat{R}_{x_ix_i}^2(1)+(-1+\rho_{x_ix_j}^2(T)))}\right\}. \tag{8}$$

Eq. (8) gives the linearized, time-delayed transfer entropy between two stationary, Gaussian processes x_i, x_j. For this special case all of the information being shared between x_i and x_j can be captured by the linear cross-correlation coefficient and the autocorrelation for $x_i(n)$.

4. Computation from time series

4.1. Mutual information

Computing the time-delayed mutual information and/or transfer entropy between two time series involves the estimation of the various probability densities that comprise Eq. (s) (2,6). It has been shown that these quantities may be obtained through use of kernel density estimation [20,22,23]. If the practitioner has access to an ensemble of measurements the densities can be estimated for non-stationary time series. However, in most SHM applications the practitioner must use a single set of measured response data. The following approach therefore assumes stationary, erogodic data. At each point in the data vector $\mathbf{x}(n)$ we form the estimate

$$\hat{p}(\mathbf{x}(n),\varepsilon) = \frac{1}{N-2t-1}\sum_{\substack{m=1\\|m-n|>t}}^{N}\Theta(\varepsilon-\|\mathbf{x}(n)-\mathbf{x}(m)\|), \tag{9}$$

where

$$\Theta(\varepsilon-\|\mathbf{x}(n)-\mathbf{x}(m)\|) = \begin{cases} 1: & \varepsilon-\|\mathbf{x}(n)-\mathbf{x}(m)\| \geqslant 0,\\ 0: & \varepsilon-\|\mathbf{x}(n)-\mathbf{x}(m)\| < 0\end{cases}$$

and the operator $\|\cdot\|$ takes the vector norm (here we use Euclidean norm). The parameter t is referred to as a Theiler window and is used to eliminate bias in the estimate due to serial correlations in the data [20]. Eq. (9) takes the local density estimate about point n to be the number of points in a hyper-sphere of size ε about that point divided by the total number of points in the time series N. Eq. (9) represents a simple form of kernel density estimation using the "step" kernel with fixed band width ε. Following Refs. [23,24] the entropy for the process $\mathbf{x}(n)$ is simply the expected value of $\log_2(p(\mathbf{x}(n)))$ and may be approximated by

$$\int p(\mathbf{x}(n))\log_2(p(\mathbf{x}(n))) \approx \frac{1}{N}\sum_n \log_2(\hat{p}(\mathbf{x}(n),\varepsilon)). \tag{10}$$

We may therefore use Eq. (10) to estimate the various Shannon entropies required of Eq. (3). For example, the mutual information requires estimates of the single and joint probability densities $\hat{p}(x_i)$, $\hat{p}(x_j)$, and $\hat{p}(x_i,x_j)$. Substituting Eq. (10) into Eq. (3) and considering a time delay in x_j gives the estimated time-delayed

mutual information

$$\hat{I}(x_i; x_j, T, \varepsilon) = \frac{1}{N}\sum_n \{\log_2(\hat{p}(x_i(n), x_j(n+T), \varepsilon)) - \log_2(\hat{p}(x_i(n), \varepsilon)) - \log_2(\hat{p}(x_j(n+T), \varepsilon))\}, \tag{11}$$

where the dependence on the ε has been left explicitly in the equation. Given two time series x_i and x_j one may compute $\hat{I}(x_i; x_j, T, \varepsilon)$ directly from the data. The above formulation is generic and may be extended to look at shared information in more than two variables or between groups of variables. This extension of mutual information is referred to in the literature as *redundancy* and is discussed thoroughly by Prichard and Theiler [23] and Paluš [25]. The algorithm for the multi-variate case stays basically the same, the only difference being that the densities must be evaluated in a higher-dimensional space. The main difficulty in implementing this scheme lies in finding near neighbors within a radius ε to a given point n. For time series of even modest size using the naive $O(N^2)$ approach is prohibitive. However, there exist a number of fast near-neighbor search algorithms available that can significantly reduce computation time. For example, the box-assisted approach of Ref. [26] or a variant of the K-D tree algorithm [27] are two frequently used options.

4.2. Transfer entropy

Transfer entropy also reduces to a simple function of the local density estimates given by Eq. (9). Using Eq. (10) to estimate the necessary entropies gives

$$\hat{\mathrm{TE}}(x_i(1)|x_i, x_j(T), \varepsilon) = \frac{1}{N}\sum_n \{\log_2(\hat{p}(x_i(n+1), x_i(n), x_j(n+T), \varepsilon)) + \log_2(\hat{p}(x_i(n), \varepsilon)) - \log_2(\hat{p}(x_i(n+1), x_i(n), \varepsilon)) - \log_2(\hat{p}(x_i(n), x_j(n+T), \varepsilon))\}. \tag{12}$$

Again dependence on the band width ε has been left in the equation. For illustrative purposes we examine the first term on the right-hand side of Eq. (12). Expanding Eq. (9) gives the needed probability density estimate as

$$\hat{p}(x_i(n+1), x_i(n), x_j(n+T), \varepsilon) = \frac{1}{N}\sum_{\substack{m=1 \\ |m-n|>t}}^{N} \Theta\left(\varepsilon - \left\| \begin{matrix} x_i(n+1) - x_i(m+1) \\ x_i(n) - x_i(m) \\ x_j(n+T) - x_j(m+T) \end{matrix} \right\|\right), \tag{13}$$

where $\|\cdot\|$ takes the Euclidean norm of the three vector components. It should be mentioned that both algorithms can also be re-written to utilized a "fixed mass" approach rather than a fixed band width. In this approach the local densities are estimated by the ratio of a fixed number of points to the volume of space occupied by those points. In this case Eq. (9) is re-written

$$\hat{p}(\mathbf{x}(n), M) = \frac{1}{N-2t-1}\frac{M}{V(\mathbf{x}(n))}, \tag{14}$$

where M is the number of nearest neighbors to look at and $V(\mathbf{x}(n))$ is the minimum volume that encompasses those points (again we exclude neighbors with in t time steps of the fiducial point n from consideration). Hyper-spheres and hyper-rectangles are two commonly used volume elements. A discussion of non-parametric density estimation techniques is given in Ref. [20]. In presenting the results we will drop the " ˆ " denoting "estimate" from both mutual information and transfer entropy.

5. Hypothesis testing: the method of surrogate data

Given two time series from a structure the practitioner may be interested in assessing whether or not the relationship between the two signals can be accurately represented by a linear model. In this section we describe one possible means of placing this question in a hypothesis testing framework using the notion of surrogate data sets. The idea behind this approach is to construct additional time series that preserve specific properties of the original data but are random with respect to other properties, presumably the ones the

practitioner is testing for. The metric(s) of interest, in this case mutual information and transfer entropy, are then computed for both surrogate data and the original data. Differences in the results indicate that the original data possesses the specific property being tested for.

In this case we are testing against the null hypothesis of a linear relationship between two, Gaussian-distributed variables. We therefore seek surrogate data sets that preserve the linear cross-correlation between x_i and x_j. One approach is to randomize the phases of the two data sets such that their difference is preserved [28]. The discrete Fourier transform of a real-valued process is given by

$$X(f) = \mathscr{F}\{x(n)\} = \sum_{n=0}^{N-1} x(n)\mathrm{e}^{-2\pi \mathrm{i} f n \Delta t},$$

where $X(f)$ is a complex-valued quantity evaluated at $f = -1/2\Delta t, \ldots, -1/N\Delta t,\ 0, 1/N\Delta t, \ldots 1/2\Delta t$. Alternatively $X(f)$ may be written in terms of a magnitude and phase as $X(f) = |X(f)|\mathrm{e}^{\mathrm{i}\phi(f)}$. The linear cross-correlation between two time records $x_1(n), x_2(n)$ may be written in the frequency domain as a product of Fourier transforms as a consequence of the Weiner–Khintchine theorem giving

$$\mathscr{F}\{R_{x_i x_j}(T)\} = 1/N\Delta t X_i(f)^* X_j(f) = 1/N\Delta t |X_i(f)||X_j(f)|\,\mathrm{e}^{\mathrm{i}(\phi_i(f)-\phi_j(f))}. \tag{15}$$

Both the magnitude of the cross-correlation and the phase relationship will remain unchanged if a random phase $\psi(f) \in [0, 2\pi)$ is added to both $\phi_i(f), \phi_j(f)$. We may therefore generate the surrogate time series $\hat{x}_i(n), \hat{x}_j(n)$ by taking

$$\hat{x}_i(n) = \mathscr{F}^{-1}\{X_i(f)\mathrm{e}^{\mathrm{i}\psi(f)}\}\ \hat{x}_j(n) = \mathscr{F}^{-1}\{X_j(f)\mathrm{e}^{\mathrm{i}\psi(f)}\}.$$

Because of the circular nature of the discrete transform the *same* random phase must be added to both positive and negative frequency components. In other words, we must set $\psi(-f) = \psi(f)$. The general algorithm for creating surrogate data sets for L time series is therefore to compute $\hat{x}_k(n) = \mathscr{F}^{-1}\{X_k(f)\mathrm{e}^{\mathrm{i}\psi}\}\ k = 1 \cdots L$. The resulting time series will exactly match *only* the linear correlations in the original data. Randomizing the phases will destroy any higher-order correlations. Utilizing either of the algorithms described by Eqs. (11) and (12) to explore relationships between the $x_i(n)$ will therefore produce different results when applied to $\hat{x}_i(n)$ in the case of nonlinear coupling. No difference means the processes are consistent with linear coupling. If the data are not Gaussian distributed a different surrogate algorithm is required that also preserves the amplitude distribution of the original data (in addition to the linear auto- and cross-correlations) [29].

6. Information flow in structures

Lets assume that our system of interest is the 5 dof spring–mass–damper depicted in Fig. 1. The equations of motion for this system are

$$\mathbf{M}\{\ddot{\mathbf{x}}\} + \mathbf{C}\{\dot{\mathbf{x}}\} + \mathbf{K}\{\mathbf{x}\} = \mathbf{f}(t), \tag{16}$$

where **M**, **C**, and **K** are the mass, damping, and stiffness matrices respectively. Let the dynamical variables of interest be the positions of the masses $x_i\ i = 1 \cdots L$. For the analysis it is convenient to work in modal

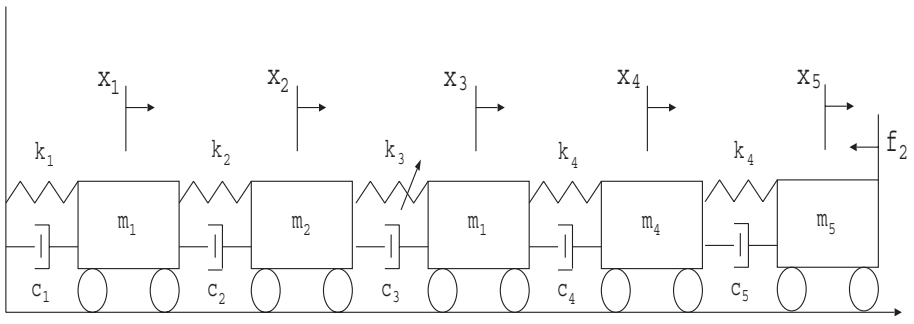

Fig. 1. Schematic of linear spring–mass–damper system.

coordinates by allowing $x_i = \sum_k^L \mathbf{u}_i \eta_k$ where $\mathbf{u}_i$ are the mass-normalized mode shapes. The decoupled equations of motion in continuous time are

$$\ddot{\eta}_i + 2\zeta_i \omega_i \dot{\eta}_i + \omega_i^2 \eta_i = \mathbf{u}_i^{\mathrm{T}} \mathbf{f}(t) = q_i(t). \tag{17}$$

Formulation of both Eqs. (4) and (8) requires the auto- and cross-correlations for the response variables. These may be derived in terms of the input (excitation) auto- and cross-correlations for the case of Gaussian excitation as

$$R_{q_l q_m}(\tau) = E[q_l(t) q_m(t+\tau)] = Q_{lm}\delta(\tau),$$

where the entries of Q_{lm} are dictated by the mode shapes, $\delta(\cdot)$ is the unit impulse, and τ is a "continuous time" measure of delay (continuous time and discrete time are related through the sampling interval Δt i.e. $\tau = T\Delta t$). For Gaussian excitation, the covariance function matrix associated with the modal forcing terms q_i is characterized by

$$Q_{lm} = (\mathbf{u}_l^{\mathrm{T}} \mathbf{f})(\mathbf{u}_m^{\mathrm{T}} \mathbf{f}). \tag{18}$$

By convolving the excitation with the impulse response for a spring–mass system

$$h_i = \frac{1}{\omega_{di}} \mathrm{e}^{\zeta_i \omega_i} \sin(\omega_{di} t) \; i = 1, \ldots, L \tag{19}$$

the response correlations may be written [30]

$$R_{x_i x_j}(\tau) = \int_0^\infty \int_0^\infty \sum_l^L \sum_m^L u_{il} u_{jm} Q_{lm} \delta(\tau + \theta_1 - \theta_2) \frac{\mathrm{e}^{[-\zeta_l \omega_l \theta_1 - \zeta_m \omega_m \theta_2]}}{\omega_{dl} \omega_{dm}} \times \sin(\omega_{dl}\theta_1) \sin(\omega_{dm}\theta_2)\, \mathrm{d}\theta_1\, \mathrm{d}\theta_2, \tag{20}$$

where $\omega_{di} \equiv \sqrt{1-\zeta_i^2}\omega_i \; i = 1, \ldots, L$ are the damped natural frequencies for the system. Carrying out the integration yields the needed correlations

$$R_{x_i x_j}(\tau) = \frac{1}{4} \sum_l^L \sum_m^L Q_{lm} u_{il} u_{jm} [A_{lm} \mathrm{e}^{-\zeta_m \omega_m \tau} \cos(\omega_{dm}\tau) + B_{lm} \mathrm{e}^{-\zeta_m \omega_m \tau} \sin(\omega_{dm}\tau)], \tag{21}$$

where

$$A_{lm} = \frac{8(\omega_l \zeta_l + \omega_m \zeta_m)}{\omega_l^4 + \omega_m^4 + 4\omega_l^3 \omega_m \zeta_l \zeta_m + 4\omega_m^3 \omega_l \zeta_l \zeta_m + 2\omega_m^2 \omega_l^2 (-1 + 2\zeta_l^2 + 2\zeta_m^2)},$$
$$B_{lm} = \frac{4(\omega_l^2 + 2\omega_l \omega_m \zeta_l \zeta_m + \omega_m^2(-1 + 2\zeta_m^2))}{\omega_{dm}(\omega_l^4 + \omega_m^4 + 4\omega_l^3 \omega_m \zeta_l \zeta_m + 4\omega_m^3 \omega_l \zeta_l \zeta_m + 2\omega_m^2 \omega_l^2 (-1 + 2\zeta_l^2 + 2\zeta_m^2))}. \tag{22}$$

Substituting into Eq. (4) or Eq. (8) along with Eqs. (21) and (22) gives a closed-form solution to both the mutual information and transfer entropy between masses i, j.

In an effort to test the algorithms we consider a linear 5 dof structure ($L = 5$) where the structure's parameters are $m_i = 0.01, c_i = 0.05, k_i = 10.0 \; i = 1 \ldots 5$. Further assume that the excitation is Gaussian (unit standard deviation) and is applied only at the end mass so that $\mathbf{f} = \{0, 0, 0, 0, \mathcal{N}(0,1)\}^{\mathrm{T}}$. The natural frequencies and damping ratios for this system are summarized in Table 1. Assuming a proportional damping model ($\mathbf{C} = \beta \mathbf{K}$) we have as an approximation $\zeta_i = (1/2) c_i \omega_i$. Using these parameters, the system described by Eq. (s) (16) was simulated using a fifth-order Runge–Kutta scheme with a time step of $\Delta t = 0.01$ s. giving time series for the displacements $x_i(n) \; n = 1 \cdots N$ where N was chosen to be 50,000 points. Prior to analysis, each time series was normalized to zero mean and unit variance.

6.1. Results: mutual information

For this analysis we focus on computing the information transport between masses $i = 2$ and $j = 3$, i.e. use $x_2(n), x_3(n)$ as the time series of interest. Fig. 2 shows the results obtained by applying Eq. (11) with $\varepsilon = 0.05$

Table 1
Modal parameters for 5 dof structure

Mode	ζ_i	ω_i (rad/s)	$\omega_i^{(A)}$ (rad/s)
1	0.02	9.0	8.8
2	0.07	26.3	25.4
3	0.10	41.4	40.0
4	0.13	53.2	51.4
5	0.15	60.7	58.7

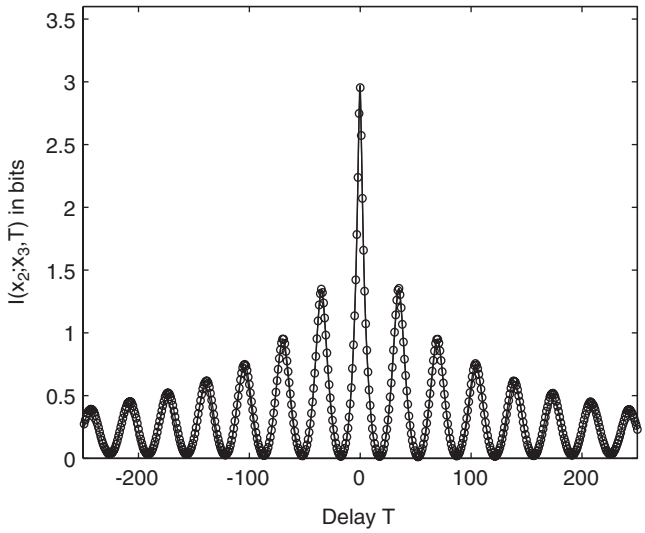

Fig. 2. Time-delayed mutual information between masses 2,3. Theoretical results (solid line) vs. simulation results (open circles).

compared with theoretical predictions obtained via Eqs. (4), (21), and (22). The kernel-based algorithm accurately captures the time-dependent correlations in the data. The dominant mode is clearly visible, however because the information fluctuates according to $\rho^2_{x_2,x_3}(T)$ the linear cross-correlation is "rectified". The period associated with the information peaks is therefore exactly half that of the dominant period. The decay of the information transport with time provides a rate of information loss. As expected, the dynamics of $x_3(T)$ say less about the dynamics $x_2(0)$ as T increases.

In an effort to demonstrate the utility of the approach in diagnosing nonlinearity a cubic spring replaces k_3 such that the linear stiffness matrix is now given by

$$\mathbf{K} = \begin{bmatrix} (k_1+k_2) & -k_2 & 0 & 0 & 0 \\ -k_2 & (k_2-k_3) & k_3 & 0 & 0 \\ 0 & k_3 & (-k_3+k_4) & -k_4 & 0 \\ 0 & 0 & -k_4 & (k_4+k_5) & -k_5 \\ 0 & 0 & 0 & -k_5 & k_5 \end{bmatrix},$$

($-k_3$ replaces k_3) and a nonlinear restoring force is added to the right-hand side of Eq. (16)

$$\mathbf{f}^{(N)} = \begin{bmatrix} 0 \\ -\mu k_3(x_3-x_2)^3 \\ \mu k_3(x_3-x_2)^3 \\ 0 \\ 0 \end{bmatrix}.$$

In the context of structural dynamics this particular nonlinearity can be used to model the behavior of a post-buckled structure [31]. The equilibrium point $x_3 - x_2 = 0$ is replaced by the two stable points $x_3 - x_2 = \pm\sqrt{1/\mu}$. As μ is increased the asymmetry in restoring force associated with the nonlinearity also increases. For a large enough value $\mu = \mu^*$ this system will begin to oscillate between the two equilibria.

Fig. 3 shows the results of computing the average mutual information function for increasing levels of nonlinearity. The curve with open circles represents the algorithm applied to the original data while the solid lines show the results of applying to the algorithm to each of ten linear surrogates, generated using the approach described in Section 5. As μ increases, the curves begin to separate, particularly near the dominant peak. The average mutual information shows an increase in the relative amount of information transmitted compared to the linear surrogates. Our interpretation is that information associated with higher-order correlations is still being transmitted, however it is "lost" when analyzing the surrogates. In order to quantify this difference we form the confidence intervals at each delay

$$\mathrm{CL}(T) = \mu(T) - Z_{\alpha/2}\sigma(T),$$

$$\mathrm{CU}(T) = \mu(T) + Z_{\alpha/2}\sigma(T),$$

where $\mu(T), \sigma(T)$ are the mean and standard deviation of the surrogates at delay T. The values for $Z_{\alpha/2}$ are chosen by the practitioner and indicate the desired level of confidence associated with the null hypothesis that the dynamics of the structure are linear. Consequently, values for the time-delayed mutual information that fall outside these bounds indicate nonlinearity (violation of the null). In this work we take $Z_{0.025} = 1.96$ giving confidence intervals of 95%. Because the ITs show an increased information transport relative to their linearized counterparts we need only focus on the upper bound. A convenient nonlinearity index for the mutual information can therefore be define based on distance from this bound as

$$Z_M = \sum_T \begin{cases} 0: & I(x_i, x_j, T) \leqslant \mathrm{CU}(T), \\ (I(x_i, x_j, T) - \mathrm{CU}(T))/\mathrm{CU}(T): & I(x_i, x_j, T) > \mathrm{CU}(T), \end{cases}$$

where we are summing over all values of the mutual information that exceed the confidence interval. An alternative is to take the maximum distance (rather than sum). We find few differences in the results regardless of which index is used. A plot of Z_M as a function of nonlinearity is shown in Fig. 4. The resulting index is monotonic with μ and quantifies the separation between the surrogates and $I(x_2, x_3, T)$. For $\mu = 0$ we have the linear system and no difference is observed between the data and the surrogates as expected. As the degree of nonlinearity is increased so too the amount of separation as quantified by Z_M. For values of $\mu > \mu^* = 1.75$ the dynamics begin to oscillate between the two equilibria and the nonlinearity is trivial to detect. Values for Z_M for this case are an order of magnitude larger than those shown in Fig. 4 and are therefore not presented. The subtle nonlinearity introduced for $\mu < \mu^*$ is much more difficult to detect and hence is the focus of this work.

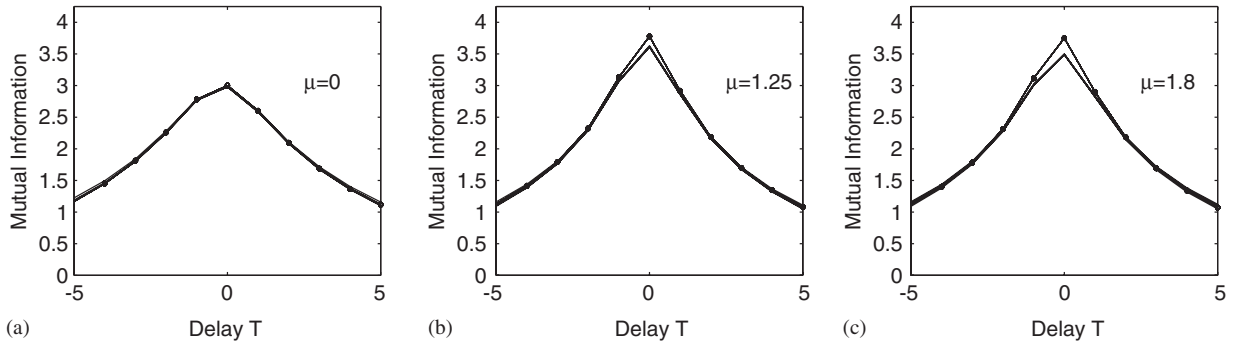

Fig. 3. Dominant peak of $I(x_2; x_3, T)$ showing increasing discrepancy between surrogates (solid line) and data (open circles) for $\mu = 0$ (linear system), $\mu = 1.5$, and 1.75.

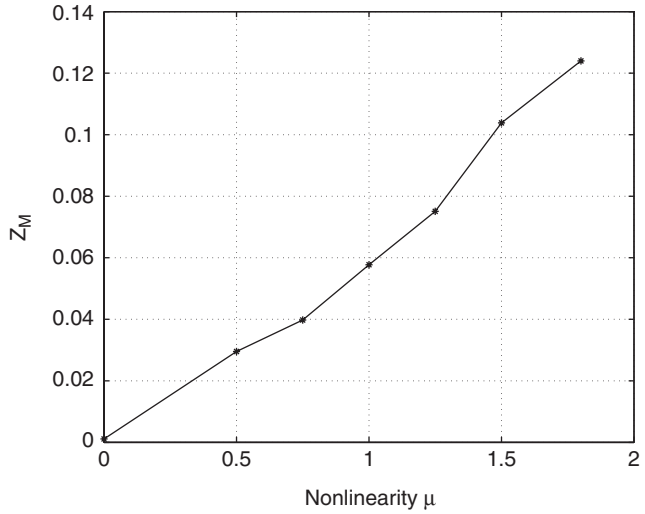

Fig. 4. Index Z_M as a function of % nonlinearity (damage) in the system.

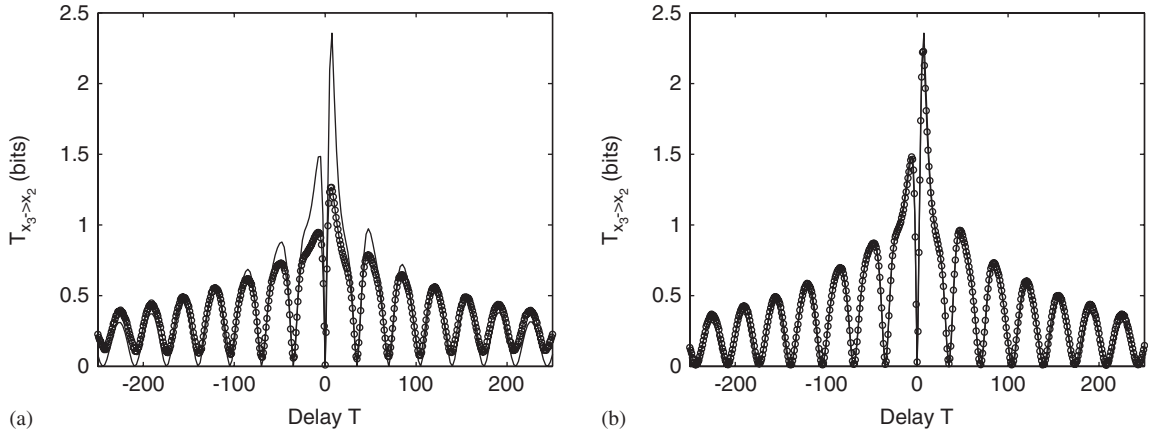

Fig. 5. Time-delayed transfer entropy between mass 3 and mass 2 based on theory (solid line) and from time series (open circles) using the algorithm based on the fixed band width kernel (a) and that based on the fixed mass kernel (b).

6.2. Results: transfer entropy

The time-delayed transfer entropy was also used in analyzing the relationship between masses 2 and 3. As an example, consider the case where we examine the information transport from x_3 to x_2, that is, compute $T_{x_3 \to x_2}$. Fig. 5 shows the analytical result for the linear system ($\mu = 0$) plotted along with the results obtained using two different approaches to estimating $T_{x_3 \to x_2}$. Fig. 5a shows the results obtained using the fixed band width kernel (Eq. (9)) with a band width of $\varepsilon = 0.075$ while Fig. 5b illustrates the fixed mass approach (Eq. (14)) based on a mass of $M = 10$ points. Only qualitative agreement was obtained between simulation and theory using the fixed band width kernel while the fixed mass approach yields a quantitative match to theory. The difficulty in obtaining good estimates via Eq. (10) likely stems from the subtle effect the transfer entropy is trying to capture. Rather than focusing on the joint density $p(x_i, x_j(T))$ (as does the mutual information), transfer entropy is attempting to capture changes in the *ratio* $p(x_i(1), x_i, x_j(T))/p(x_i, x_j(T))$. For systems that possess significant auto-correlation, this ratio will be small; this can be seen by examining the numerator of Eq. (8). Trying to capture these subtle differences in densities using a relatively crude density

estimation technique is likely the cause of the discrepancy between numerics and theory. The fixed mass kernel, on the other hand, is adaptive and effectively adjusts to maintain a constant density of points. This estimator therefore tends to be more accurate. The problem with the fixed mass estimator is that it carries a greater computational cost (finding the *M nearest* neighbors is inherently more difficult than finding all neighbors within a radius ε). For the application presented in this work (detecting differences between surrogates and data) both estimators led to nearly identical results for several test cases. We therefore utilized the more computationally efficient fixed band width kernel for the remainder of the study and take $\varepsilon = 0.075$. We point out that results are largely insensitive to this choice. Any value for ε between 2.5% and 12.5% of the standard deviation of the time series works well.

As with mutual information, results can be compared to those obtained from surrogate data as nonlinearity is introduced into the system. Fig. 6 illustrates these results for several different values of the nonlinearity parameter μ. The transfer entropy appears more sensitive to increasing nonlinearity then does the mutual information. Furthermore, the differences between surrogates and data are noticeable over a wider range of delay T. As with the mutual information we may define a nonlinearity index (Fig. 7)

$$Z_T = \sum_T \begin{cases} 0: & T(x_i(1)|x_i, x_j, T) \leqslant \mathrm{CU}(T), \\ (T(x_i(1)|x_i, x_j, T) - \mathrm{CU}(T))/\mathrm{CU}(T): & T(x_i(1)|x_i, x_j, T) > \mathrm{CU}(T), \end{cases}$$

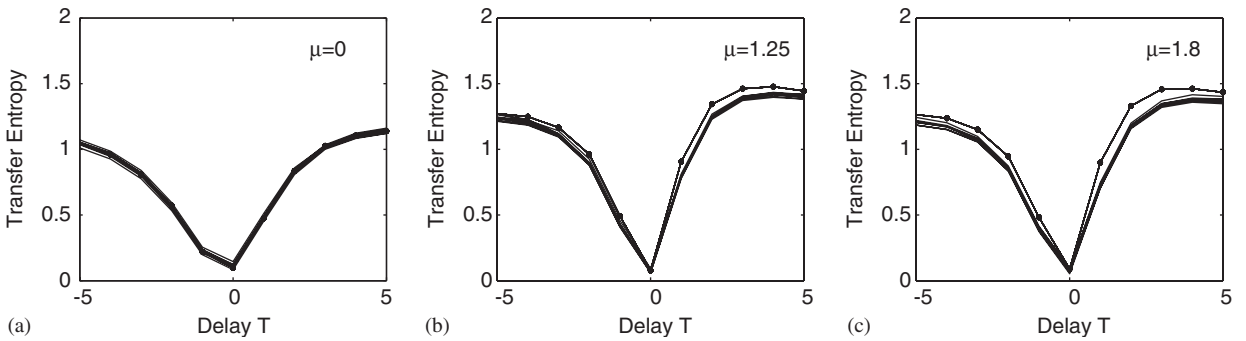

Fig. 6. Plot of $T_{x_3 \to x_2}$ showing increasing discrepancy between surrogates (solid line) and data (open circles) for $\mu = 0$ (linear system), $\mu = 1.5$, and 1.75.

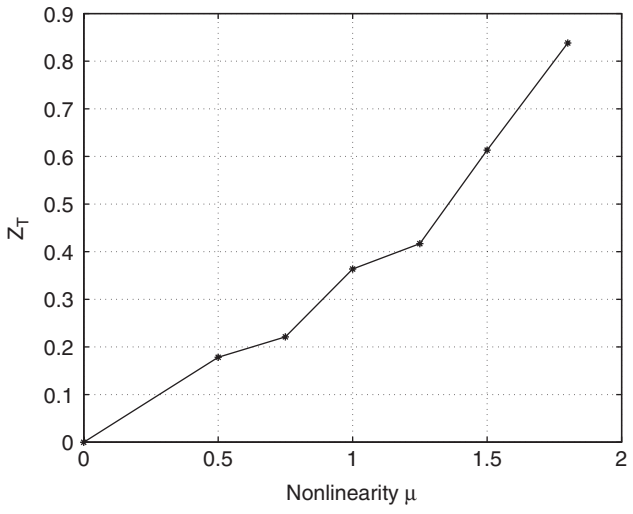

Fig. 7. Index Z_T as a function of % nonlinearity (damage) in the system.

where again the upper confidence limit CU(T) is chosen based on the mean and standard deviation of surrogate values for delay T. The values of this index are larger than are those for the mutual information. This is consistent with other model systems we have examined. We conclude that for this simple system, transfer entropy is a more sensitive indicator of nonlinear coupling.

6.3. Invariance to ambient variation

Perhaps the greatest strength of the proposed approach is that it is insensitive to certain types of ambient variability such as those caused by temperature, humidity, etc. Unless these changes affect the *form* of the underlying dynamics (linear/nonlinear) they will not affect the proposed indicators Z_M, Z_T. In an effort to demonstrate this, the stiffness values were altered to simulate a temperature gradient across the structure. This was accomplished by decreasing the first stiffness value by 2%, the next by 4% and so on. The last stiffness, k_5, was therefore altered by 10%. Again we explore the relationship between x_2, x_3 using both the original simulated time series and ten linear surrogates. Sample results are displayed in Fig. 8 for both mutual information and transfer entropy in the case of $\mu = 1.45$. Again we can see a clear difference between the surrogates and the data indicating that there is a statistically significant degree of nonlinearity in the structure. Although the global stiffness properties have changed, the nonlinearity remains. The natural frequencies for the altered structure, denoted $\omega_i^{(A)}$, are summarized in Table 1.

Damage indices were computed in the same manner as in the previous example and the results are displayed in Fig. 9. As the level of nonlinearity is increased both indices rise in monotonic fashion. The main difference is

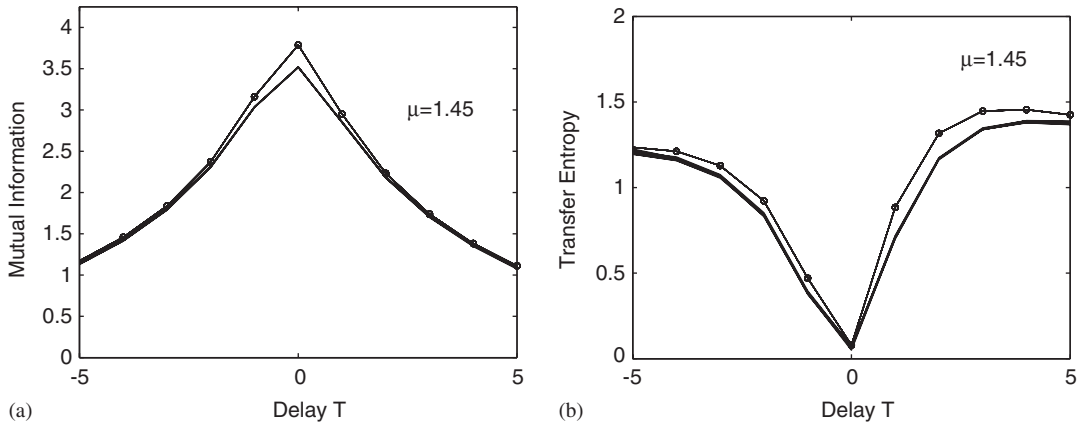

Fig. 8. Mutual information (left) and transfer entropy (right) for the case where $\mu = 1.45$.

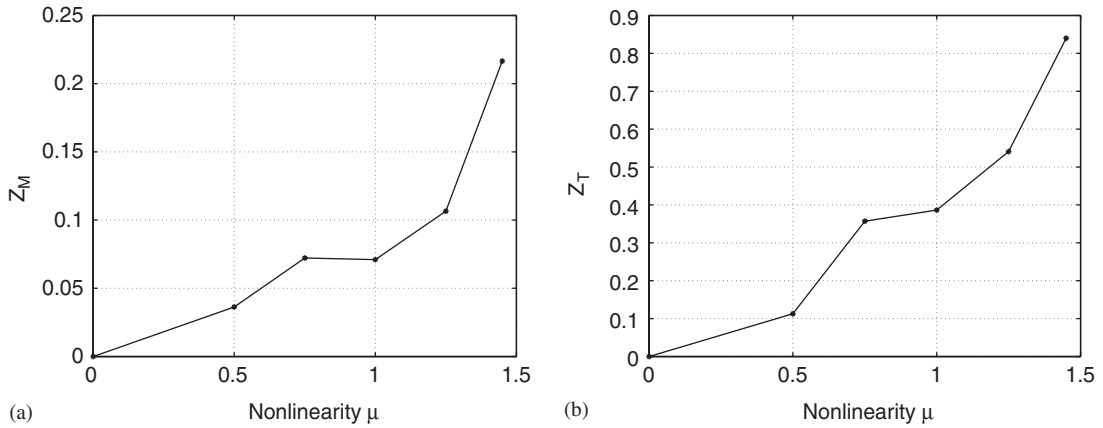

Fig. 9. Damage indices Z_M, Z_T as a function of % nonlinearity (damage) in the system.

that the values of both indices are slightly higher than in the previous case. For example, in the original structure $Z_T = 0.8$ for $\mu = 1.75$ while here $Z_T = 0.8$ for $\mu = 1.45$. This can be explained by the fact that the perturbed stiffness values have changed the point at which the system begins to oscillate between the two equilibria. Given our fixed level of excitation (Gaussian noise with unit standard deviation), these oscillations now occur for values $\mu > \mu^* = 1.45$ (as opposed to $\mu^* = 1.75$) and the nonlinearity becomes trivial to detect as before. Differences in the progression of Z_M, Z_T with damage from the previous case (no temperature gradient) can at least partially be explained in terms of the number of surrogate data sets used. In this study we utilized ten surrogates. Because Z_M, Z_T are based on the variance of the surrogates, larger numbers of surrogates tend to produce a "smoother", more reliable progression. However, the computation time increases with the addition of each surrogate set. Choice of number of surrogates will likely be application specific. For illustrative purposes ten surrogate sets were deemed sufficient. The important feature to note in Fig. 9 is that the damage index for the linear structure remains zero even though the natural frequencies of the structure have shifted by between 2.2% and 5% (depending on the mode). Mode shapes for the structure are similarly altered. Health monitoring schemes based on modal properties would, in this example, produce false positives (declare damage when none exists) or suffer a reduced sensitivity to the damage. We stress that this approach yields an absolute measure of nonlinearity as opposed to relative. This approach therefore obviates the need for baseline data sets for feature comparisons. We still require a baseline *assumption* equating "healthy" with linear, but no baseline time series. The surrogates are, in effect, a baseline (null hypothesis) against which the hypothesis of nonlinearity may be tested. A structure that has been retro-fitted with a health monitoring system (sensors/algorithms) and for which no baseline exists could still be monitored for damage.

The main strengths of the described approach pre-suppose that damage takes the form of a nonlinearity. However, if this is not the case (i.e linear damage or a healthy structure who's dynamics are nonlinear) the approach can still be utilized by drawing comparisons between IT metrics computed from a baseline data set and a damaged data set. In this case there would be no need for surrogates, however, as a true baseline would be required. As we have demonstrated (see Eqs. (4) and (8)), in the limiting case of a linear structure the IT metrics carry the same information as does the linear auto- and cross-correlation functions and (by the Weiner–Khintchine theorem) the auto- and cross-spectral densities. Their use in the case of linear damage is therefore tantamount to looking for changes in linear properties such as modal frequencies.

7. Conclusions

In this work we have described a process by which the vibrational response of a structure can be analyzed for the presence of nonlinearity. Both the time-delayed mutual information and time-delayed transfer entropy were presented as two alternative, probabilistic definitions of coupling. In contrast to standard signal processing techniques which focus on second-order (linear) correlations, these two quantities capture coupling in all moments of the signal's underlying probability density functions. Because both quantities capture general dependencies among time series they may be effectively used to diagnose when the coupling is nonlinear. We have demonstrated an approach by which the practitioner constructs surrogate data sets that preserve the second-order correlations in the data but that destroy any higher-order correlations. Computing either mutual information or transfer entropy on both the actual data and the surrogates was shown to produce different results when nonlinearity was present. A nonlinearity index for capturing this difference was introduced and showed a monotonic increase with the degree of system nonlinearity. With regard to SHM, this approach eliminates both the necessity of acquiring baseline statistics and the problems associated with separating ambient variation from damage. With regard to the former, the proposed technique provides an absolute measure of nonlinearity in the system and therefore does not require the comparison to a baseline data set. This has recently been demonstrated for two different experimental systems [32,33]. Furthermore, because the proposed approach seeks a direct measure of nonlinearity, global changes in system properties such as stiffness will not affect the results. Here we have demonstrated this by changing the stiffness values of the structure to simulate a temperature gradient. The nonlinearity indices for both mutual information and transfer entropy were largely insensitive to this change.

References

[1] B. Peeters, J. Maeck, G.D. Roeck, Vibration-based damage detection in civil engineering: excitation sources and temperature effects, *Smart Materials and Structures* 10 (3) (2001) 518–527.

[2] L.-A. Wong, J.-C. Chen, Damage identification of nonlinear structural systems, *AIAA Journal* 38 (8) (2000) 1444–1452.

[3] T.J. Johnson, D.E. Adams, Transmissibility as a differential indicator of structural damage, *Journal of Vibration and Acoustics* 124 (2002) 634–641.

[4] K. Worden, G.R. Tomlinson, Nonlinearity in experimental modal analysis, *Philosophical Transactions of the Royal Society A* 359 (2001) 113–130.

[5] S.A. Neild, M.S. Williams, P.D. McFadden, Nonlinear vibration characteristics of damaged concrete beams, *Journal of Structural Engineering* 129 (2) (2003) 260–268.

[6] M. Feldman, Nonlinear system vibration analysis using hilbert transform—i: free vibration analysis method "freevib", *Mechanical Systems and Signal Processing* 8 (2) (1994) 119–127.

[7] M. Feldman, Nonlinear system vibration analysis using hilbert transform—ii: forced vibration analysis method "forcevib", *Mechanical Systems and Signal Processing* 8 (3) (1994) 309–318.

[8] M. Feldman, S. Seibold, Damage diagnosis of rotors: application of hilbert transform and multihypothesis testing, *Journal of Vibration and Control* 5 (3) (1999) 421–442.

[9] W.J. Staszewski, Identification of non-linear systems using multi-scale ridges and skeletons of the wavelet transform, *Journal of Sound and Vibration* 214 (4) (1998) 639–658.

[10] G. Kerschen, J.-C. Gonlival, F.M. Hemez, Bayesian model screening for the identification of nonlinear mechanical structures, *Journal of Vibration and Acoustics* 125 (2003) 389–397.

[11] A.M. Fraser, H.L. Swinney, Independent coordinates for strange attractors from mutual information, *Physical Review A* 33 (1986) 1134–1140.

[12] H.V.B.I. Trendafilova, W. Heylen, Measurement point selection in damage detection using the mutual information concept, *Smart Materials and Structures* 10 (3) (2001) 528–533.

[13] O. Oyman, R.U. Nabar, H. Bölcskei, A.J. Paulraj, Characterizing the statistical properties of mutual information in mimo channels, *IEEE Transactions on Signal Processing* 51 (11) (2003) 2784–2795.

[14] P. Comon, Independent component analysis, a new concept?, *Signal Processing* 36 (1994) 287–314.

[15] J.A. Vastano, H.L. Swinney, Information transport in spatiotemporal systems, *Physical Review Letters* 60 (18) (1988) 1773–1776.

[16] A. Destexhe, Oscillations, complex spatiotemporal behavior, and information transport in networks of excitatory and inhibitory neurons, *Physical Review E* 50 (2) (1994) 1594–1606.

[17] M.C. Ho, F.C. Shin, Information flow and nontrivial collective behavior in chaotic-coupled-map lattices, *Physical Review E* 67 (5) (2003) 056214.

[18] J.M. Nichols, Inferences about information flow and dispersal for spatially extended population systems using time series data, *Proceedings of the Royal Society of London - Biological Sciences* 272 (1565) (2005) 871–876.

[19] T. Schreiber, Measuring information transfer, *Physical Review Letters* 85 (2000) 461.

[20] A. Kaiser, T. Schreiber, Information transfer in continuous processes, *Physica D* 166 (2002) 43–62.

[21] R. Marschinski, H. Kantz, Analysing the information flow between financial time series, *European Physical Journal B* 30 (2002) 275–281.

[22] B.W. Silverman, *Density Estimation for Statistics and Data Analysis*, Chapman & Hall, London, 1986.

[23] D. Prichard, J. Theiler, Generalized redundancies for time series analysis, *Physica D* 84 (1995) 476–493.

[24] W. Liebert, H.G. Schuster, Proper choice of the time delay for the analysis of chaotic time series, *Physics Letters A* 142 (1989) 107–111.

[25] M. Paluš, Testing for nonlinearity using redundancies: quantitative and qualitative aspects, *Physica D* 80 (1995) 186–205.

[26] P. Grassberger, An optimized box-assisted algorithm for fractal dimensions, *Physics Letters A* 148 (1990) 63–68.

[27] J.L. Bentley, Multidimensional binary search trees in database applications, *IEEE Transactions on Software Engineering* SE-5 (4) (1979) 333–340.

[28] D. Prichard, J. Theiler, Generating surrogate data for time series with several simultaneously measured variables, *Physical Review Letters* 73 (7) (1994) 951–954.

[29] T. Schreiber, A. Schmitz, Improved surrogate data for nonlinearity tests, *Physical Review Letters* 77 (4) (1996) 635–638.

[30] H. Benaroya, *Mechanical Vibration: Analysis, Uncertainties, and Control*, Prentice-Hall, Englewood Chiffs, NJ, 1998.

[31] L.N. Virgin, *Introduction to Experimental Nonlinear Dynamics: A Case Study in Mechanical Vibration*, Cambridge University Press, Cambridge, 2000.

[32] J.M. Nichols, M. Seaver, S.T. Trickey, L.W. Salvino, D.L. Pecora, Detecting impact damage in experimental composite structures: an information-theoretic approach, *Smart Materials and Structures* 14 (2005) 1–11.

[33] J.M. Nichols, M. Seaver, S.T. Trickey, T. Bash, M. Kasarda, Use of information theory in structural monitoring applications, in: F.-K. Chang (Ed.), *Proceedings of the Fifth International Workshop on Structural Health Monitoring*, DEStech Publications, Lancaster, PA, 2005.